HHS Public Access

Author manuscript

Nano Lett. Author manuscript; available in PMC 2021 July 29.

Published in final edited form as:

Nano Lett. 2021 March 24; 21(6): 2461–2469. doi:10.1021/acs.nanolett.0c04759.

A Cationic Metal–Organic Framework to Scavenge Cell-Free DNA for Severe Sepsis Management

Feng Liu[○],

Key Laboratory of Polymer Ecomaterials, Changchun Institute of Applied Chemistry, Chinese Academy of Sciences, Changchun 130022, China; Department of Biomedical Engineering, Columbia University, New York City, New York 10027, United States; University of Chinese Academy of Sciences, Beijing 100049, China

Shu Sheng[○],

Key Laboratory of Polymer Ecomaterials, Changchun Institute of Applied Chemistry, Chinese Academy of Sciences, Changchun 130022, China; University of Chinese Academy of Sciences, Beijing 100049, China

Dan Shao,

Institutes for Life Sciences, School of Biomedical Sciences and Engineering, South China University of Technology, Guangzhou 510006, China

Yongqiang Xiao,

Department of Biomedical Engineering, Columbia University, New York City, New York 10027, United States

Yiling Zhong,

Department of Biomedical Engineering, Columbia University, New York City, New York 10027, United States

Jie Zhou,

Department of Biomedical Engineering, Columbia University, New York City, New York 10027, United States

Chai Hoon Quek,

Corresponding Authors liyanhui@ciac.ac.cn, thy@ciac.ac.cn, kam.leong@columbia.edu.

[○]Author Contributions

F.L. and S.S. contributed equally to this work. The manuscript was written through contributions of all authors. All authors have given approval to the final version of the manuscript.

The authors declare no competing financial interest.

Supporting Information

The Supporting Information is available free of charge at https://pubs.acs.org/doi/10.1021/acs.nanolett.0c04759.

Materials and methods; (Figure S1) characterization of materials; (Figure S2) BET surface area result of NPs; (Figure S3) TGA analysis of NPs; (Figure S4) schematic of activation of HEK-Blue hTLR reporter cells by agonists; (Figure S5) activation of HEK-Blue hTLR9, hTLR3, and hTLR4 reporter cells by materals (no agonists added); (Figure S6) activation of (A) HEK-Blue hTLR9 and (B) hTLR4 cells after treatment of ZIF-8 with different weight ratio to agonists; (Figure S7) ROS level of cells from the peritoneal cavity of mice in different treatment groups; (Figure S8) H&E staining images of major organs of mice in different treatment groups; (Figure S9) blood biochemistry analysis of mice in different treatment groups; (Figure S10) H&E staining images of major organs of mice after injection with free PEI 1800 and PEI 1800-*g*-ZIF NPs for 5 days; and (Table S1) Zn content analysis of ZIF-8 and PEI-*g*-ZIF NPs (PDF)

Complete contact information is available at: https://pubs.acs.org/10.1021/acs.nanolett.0c04759

Department of Biomedical Engineering, Columbia University, New York City, New York 10027, United States

Yanbing Wang,
Key Laboratory of Polymer Ecomaterials, Changchun Institute of Applied Chemistry, Chinese Academy of Sciences, Changchun 130022, China; University of Science and Technology of China, Hefei 230026, China

Zhiming Hu,
Key Laboratory of Polymer Ecomaterials, Changchun Institute of Applied Chemistry, Chinese Academy of Sciences, Changchun 130022, China

Heshi Liu,
Key Laboratory of Polymer Ecomaterials, Changchun Institute of Applied Chemistry, Chinese Academy of Sciences, Changchun 130022, China

Yanhui Li,
School of Materials Science and Engineering, Changchun University of Science and Technology, Changchun 130022, China

Huayu Tian,
Key Laboratory of Polymer Ecomaterials, Changchun Institute of Applied Chemistry, Chinese Academy of Sciences, Changchun 130022, China; University of Chinese Academy of Sciences, Beijing 100049, China; University of Science and Technology of China, Hefei 230026, China

Kam W. Leong,
Department of Biomedical Engineering, Columbia University, New York City, New York 10027, United States

Xuesi Chen
Key Laboratory of Polymer Ecomaterials, Changchun Institute of Applied Chemistry, Chinese Academy of Sciences, Changchun 130022, China; University of Chinese Academy of Sciences, Beijing 100049, China; University of Science and Technology of China, Hefei 230026, China

Abstract

Circulating cell-free DNA (cfDNA) released by damaged cells causes inflammation and has been associated with the progression of sepsis. One proposed strategy to treat sepsis is to scavenge this inflammatory circulating cfDNA. Here, we develop a cfDNA-scavenging nanoparticle (NP) that consists of cationic polyethylenimine (PEI) of different molecular weight grafted to zeolitic imidazolate framework-8 (PEI-*g*-ZIF) in a simple one-pot process. PEI-*g*-ZIF NPs fabricated using PEI 1800 and PEI 25k but not PEI 600 suppressed cfDNA-induced TLR activation and subsequent nuclear factor kappa B pathway activity. PEI 1800-*g*-ZIF NPs showed greater inhibition of cfDNA-associated inflammation and multiple organ injury than naked PEI 1800 (lacking ZIF), and had greater therapeutic efficacy in treating sepsis. These results indicate that PEI-*g*-ZIF NPs acts as a “nanotrap” that improves upon naked PEI in scavenging circulating cfDNA, reducing inflammation, and reversing the progression of sepsis, thus providing a novel strategy for sepsis treatment.

Graphical Abstract

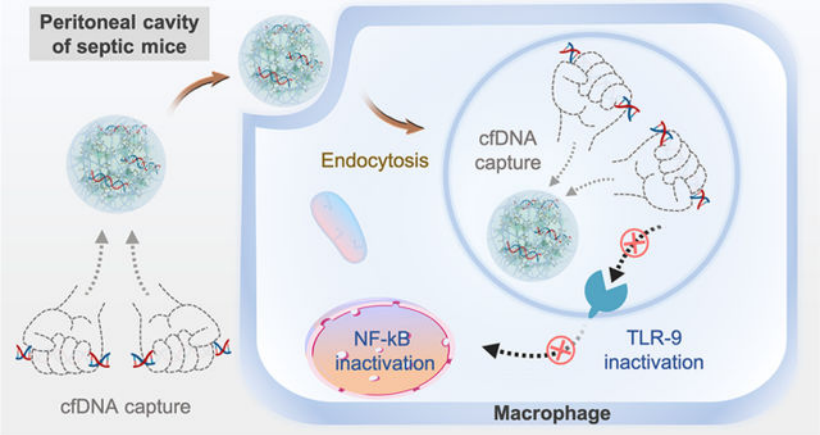

Keywords

sepsis; cell-free DNA; metal−organic framework; polyethylenimine; nanotrap

INTRODUCTION

Sepsis is a life-threatening systemic inflammatory response to infection[1,2] that involves a dysregulated host immune response and aberrant inflammatory reactions which can lead to multiple organ damage and death.[3–5] The WHO estimates that nearly 20% of all deaths globally are caused by sepsis.[6] Treatments for sepsis include administration of intravenous fluids for fluid and metabolic resuscitation, antibiotics, removal of endotoxins using polymyxin B columns, and anti-inflammatory corticosteroids or anticytokine drugs.[7–9] However, the mortality rate for severe sepsis remains as high as 50% in some settings, and as high as 80% for septic shock,[6] and there is an urgent need for more effective sepsis therapies.

Inflammatory dysregulation in sepsis is driven by activation of pattern recognition receptors (PRRs). During sepsis progression, PRRs such as toll-like receptors (TLRs) play an essential role in the aberrant inflammatory response that contributes to sepsis-related mortality.[10] In sepsis, the host immune response is initiated by PRR recognition of danger signals such as pathogen-associated molecular patterns (PAMPs) or endogenous danger-associated molecular patterns (DAMPs).[11,12] Cell-free DNA (cfDNA)–which includes pathogen-derived CpG oligodeoxynucleotides, endogenous DNA released by damaged cells, and neutrophil extracellular traps–is thought to play a critical role in eliciting a sterile inflammatory response during sepsis.[13] cfDNA is recognized by TLRs, evoking intracellular signaling cascades that activate transcription factors including nuclear factor kappa B (NF-κB), eliciting inflammatory cytokine expression.[14] Two main strategies have been explored for blocking TLR activation by cfDNA, i.e., (1) the use of TLR antagonists and (2) clearance of inflammatory circulating cfDNA. Many antagonists have been developed to block TLR activation to treat inflammation-related diseases.[15,16] However, these antagonists systemically inhibit TLR function, which can result in immune suppression and increase the risk of infection.[17] An alternative is to use cationic nanoparticles (NPs) to bind and eliminate

the anionic proinflammatory nucleic acids such as CpG. Cationic NPs have been shown to scavenge cfDNA, have exhibited therapeutic efficacy in a mouse liver failure model,[18] and have shown beneficial effects in treating cancer metastasis, rheumatoid arthritis, and lupus–diseases that involve pathological immune responses and TLR activation.[19–22] Thus, using cationic NPs to scavenge inflammatory cfDNA is a promising approach for preventing aberrant TLR activation and to treat sepsis without blocking all TLR function.

Here, we create cationic metal−organic "nanotraps" for scavenging inflammatory circulating DNA by grafting cationic polyethylenimine (PEI) polymers onto a zeolitic imidazolate framework-8 (PEI-*g*-ZIF) via a simple one-pot process (Figure 1A). We compare PEI-*g*-ZIF NPs fabricated using PEI of different molecular weights (600, 1800, and 25k Da) and with pure PEI (lacking ZIF), and characterize the NPs in terms of their composition and physiochemical properties, DNA binding affinity, inhibition of cfDNA-induced TLR activation and inflammatory cytokine release, and antisepsis therapeutic activity in a cecal ligation and puncture (CLP)-induced sepsis model *in vivo* (Figure 1B and 1C).

RESULTS AND DISCUSSION

Characterization of NPs.

PEI-*g*-ZIF NPs were synthesized *in situ* by mixing 2-methylimidazole (MIM), Zn^{2+}, and PEI of different molecular weights (600, 1800, and 25k Da) using a simple, rapid method at ambient temperature (see Experimental Procedures). PEI molecules coordinate with Zn^{2+} and serve as linkers with MIM during synthesis, endowing the NPs with positive charge and excellent dispersibility in aqueous solution. The assembly of Zn^{2+}, MIM, and PEI during the synthesis process could be deduced in two modes. One is that PEI embedded into the framework through Zn−N bonds, and the other is tangling onto the particle surface through Zn−N bonds. The size and polydispersity index (PDI) of the NPs decreased with increasing PEI molecular weight (Figure S1A–C), possibly due to preferential coordination of PEI amino groups with Zn^{2+} over the excess MIM, causing accelerated formation of smaller PEI-*g*-ZIF NPs. The strong electrostatic repulsive force and soluble amine groups provided by PEI resulted in high dispersity. The effect of PEI on particle composition was investigated by Fourier transform infrared (FTIR) spectroscopy and ^{1}H nuclear magnetic resonance (NMR) spectroscopy. A weakened absorption peak at 421 cm^{-1} belonging to the Zn−N stretch vibration of ZIF-8 was observed in the FTIR spectra of PEI-*g*-ZIF NPs (Figure S1D),[23] suggesting that reduced formation of Zn−MIM−Zn bonds resulted from coordination between PEI and Zn. In addition, a new broad peak around 3000−3700 cm^{-1} assigned to N−H stretching vibration of primary and secondary amino groups of PEI appeared in the spectra of PEI 1800-*g*-ZIF and PEI 25k-*g*-ZIF NPs but not in the spectrum of pure ZIF-8 NPs, indicating successful grafting of PEI. The appearance of a proton peak belonging to PEI at 3.0−4.0 ppm in ^{1}H NMR spectra confirmed the existence of PEI in PEI 1800-*g*-ZIF and PEI 25k-*g*-ZIF NPs (Figure S1E).[24] Interestingly, a negligible peak belonging to PEI was observed in the FTIR and ^{1}H NMR spectra of PEI 600-*g*-ZIF NPs, possibly due to the small amount of PEI in these NPs. A major ZIF-8 crystalline peak was observed in the powder X-ray diffraction (PXRD) spectrum of the PEI-*g*-ZIF NPs, indicating the preservation of ZIF-8 structure after introduction of PEI. The reduced peaks in PEI-*g*-ZIF

NPs compared with pure ZIF-8 NPs could be interpreted as reduced crystallinity after grafting PEI (Figure S1F).[25] The Brunauer−Emmett−Teller (BET) surface area of PEI 1800-*g*-ZIF NPs and PEI 25k-*g*-ZIF NPs decreased to 110.4 and 38.2 m^2/g compared with that of 1566 m^2/g for ZIF-8 NPs (Figure S2), which could be ascribed to the insertion of significant quantities of PEI molecule into the pores as well as nonporous polymer material coated on the external surface. The amounts of PEI and Zn in the PEI-*g*-ZIF NPs were determined by thermogravimetric analysis (TGA) and by inductively coupled plasma mass spectrometry (ICP-MS) (Figure S3 and Table S1).

DNA Binding Affinity of Cationic NPs.

The DNA binding affinity of the cationic NPs was investigated by competitive binding of calf thymus DNA with PicoGreen agent in TE buffer with and without 10% FBS. All cationic NPs except PEI 600-*g*-ZIF showed excellent DNA binding affinity, even at low NPs:DNA weight ratios (Figure 2A). PEI 1800-*g*-ZIF and PEI 25k-*g*-ZIF NPs exhibited greater DNA binding affinity than PEI 600-*g*-ZIF NPs, indicating that DNA binding was influenced by the PEI molecular weight. Encouragingly, PEI 1800-*g*-ZIF and PEI 25k-*g*-ZIF NPs showed similar DNA binding affinity as their pure PEI counterparts (PEI 1800 and PEI 25k), despite the lower density of PEI on their surfaces. The presence of 10% FBS reduced DNA binding in all groups at a low NPs:DNA weight ratio (Figure 2B), possibly due to FBS proteins competitively binding the DNA or the NPs, but DNA binding was restored at higher NPs:DNA weight ratios. A heparin competition array was conducted to investigate the stability of the NPs−DNA complex. DNA binding affinity was unaffected at heparin:DNA weight ratios less than 3.2 but decreased at higher heparin:DNA weight ratios (Figure 2C). Taken together, these results indicated that the cationic NPs could bind DNA in the presence of serum at moderate NPs concentrations.

TLR9 is expressed not only on the plasma membrane but also in cell endosomes.[26] As CpG oligonucleotides are internalized by endocytosis, TLR9 is relocated to the CpG-containing endosomes. Colocalization of CpG DNA and TLR9 in endosomes induces recruitment of the adapter protein MYD88 to initiate signaling.[27] Therefore, we conducted an intracellular trafficking *in vitro* study using FITC-labeled PEI-*g*-ZIF NPs and Cy5-labeled CpG 1826 to investigate endocytosis of the NPs and their potential to bind CpG and block TLR9 activation. A CCK-8 assay was performed to determine NPs cytotoxicity, and an NPs concentration of 10 μg/mL was selected for subsequent experiments as PEI-*g*-ZIF NPs exhibited limited cytotoxicity to RAW 264.7 at concentrations below 12.5 μg/mL (Figure 2D). Colocalization of PEI-*g*-ZIF NPs and CpG fluorescence was observed in endolysosomes (Figure 2E), indicating internalization of PEI-*g*-ZIF NPs via endocytosis, which might be beneficial for blocking recognition between CpG and TLR9 and reducing inflammation in sepsis.

Anti-inflammatory Effect *In Vitro*.

We next evaluated the ability of the NPs to reduce cfDNA-induced inflammation *in vitro*. The ability of the NPs to block cfDNA-induced TLR activation was evaluated by using HEK-Blue human TLRs (hTLRs) cells and monitoring the downstream activation of NF-κB. HEK-Blue hTLRs cells were constructed by cotransfection of the hTLRs gene and an

optimized secreted embryonic alkaline phosphatase (SEAP) reporter gene into HEK 293 cells. The expression of the SEAP reporter gene was controlled by an IFN-β minimal promoter fused to five NF-κB and AP-1 binding sites. Stimulation with TLR agonists activates NF-κB and AP-1, which induces SEAP expression (Figure S4). SEAP expression levels were determined by using OD at 620 nm. The cationic NPs alone showed negligible influence on TLRs pathway (Figure S5). ZIF-8 NPs with different concentration displayed negligible inhibitory effect on the CpG-induced TLR9 activation and LPS-induced TLR4 activation (Figure S6). All cationic NPs except PEI 600-*g*-ZIF reduced CpG-induced activation of HEK-Blue hTLR9 cells and poly(I:C)-induced activation HEK-Blue hTLR3 cells in a dose-dependent manner. Consistent with the DNA binding results, PEI 1800-*g*-ZIF and PEI 25k-*g*-ZIF NPs showed an inhibition effect that was similar to that of pure PEI 1800 and PEI 25k (Figure 3A, B, D, E). In contrast, lipopolysaccharide (LPS)-induced HEK-Blue hTLR4 cell activation was not affected even at a high NPs:DNA weight ratio of 10000/1 (Figure 3C, F), indicating that the cationic NPs specifically block cfDNA-induced TLR activation and subsequent NF-κB expression (Figure 3G). Previously, TLR9 activation and inflammatory cytokine secretion was observed a cecal ligation and puncture (CLP)-induced mice sepsis model.[28] Therefore, we cocultured CpG with RAW 264.7 macrophages to induce TLR9 activation to investigate the anti-inflammatory effect of the cationic NPs. Transcription of tumor necrosis factor-α (TNF-α) mRNA and expression of TNF-α cytokine both increased significantly after 24 h of coculture of the CpG and the macrophages (Figure 3H, I). Addition of cationic NPs inhibited macrophage activation and TNF-α release, demonstrating an anti-inflammation effect due to DNA binding by the NPs.

Therapeutic Effect of Cationic NPs in the CLP Model of Sepsis.

Having confirmed that the cationic NPs block TLR9 activation and reduce NF-κB and TNF-α expression *in vitro*, we turned our attention to investigate the therapeutic activity of the NPs *in vivo*. The CLP model (Figure 4A), which involves polymicrobial peritonitis-induced sepsis, is widely used to study sepsis and exhibits activation of TLRs and other characteristics relevant to clinical sepsis. We chose PEI 1800-*g*-ZIF NPs for the *in vivo* study due to the negligible DNA scavenging by PEI 600-*g*-ZIF NPs and the previously reported severe systemic toxicity of PEI 25k.[28] We compared the PEI 1800-*g*-ZIF NPs to pure PEI 1800. A CLP model with high-grade sepsis was established in C57 mice. The survival rate, clinical score, and body weight of mice in different treatment groups were monitored for five consecutive days after CLP-induced sepsis. All animals in the untreated CLP group died within 48 h. In contrast, intraperitoneal (i.p.) administration of PEI 1800-*g*-ZIF NPs at 1 and 12 h post-CLP produced a survival rate of 50%, higher than that of the pure PEI 1800-treated group (30%), and otherwise delayed sepsis-induced death (Figure 4B). A significantly reduced clinical score was observed in the pure PEI 1800 and PEI 1800-*g*-ZIF NPs treatment groups, indicating restoration of physical and mental states after treatment (Figure 4C), which was further validated by the increase in body weight after 2 days of treatment with the materials (Figure 4D). The biodistribution of pure PEI 1800 and PEI 1800-*g*-ZIF NPs was assessed by labeling the materials with Cy7 and using *ex vivo* fluorescence imaging. Following injection with materials at 1 h after CLP, the major organs and cecum were harvested at 4, 12, and 24 h after CLP for fluorescence imaging. Both Cy7-labeled pure PEI 1800 and PEI 1800-*g*-ZIF NPs preferentially localized in the liver and

inflamed cecum of CLP mice (Figure 4E, F). Accumulation of cationic NPs increased with time and reached a peak at 12 h, then decreased subsequently. The PEI 1800-*g*-ZIF NPs exhibited a longer retention time in major organs than the pure PEI 1800, which may result in prolonged protection from inflammatory cfDNA released by damaged organs.

The amount of cfDNA in serum sharply increased after establishment of CLP compared with control and sham groups. Notably, PEI 1800-*g*-ZIF NPs and PEI 1800 treatments reduced the cfDNA level to the normal level (Figure 5A, B), consistent with the *in vitro* DNA binding results, confirming the cfDNA scavenging ability of the materials *in vivo*. We also investigated the level of reactive oxygen species (ROS), as excessive production of harmful ROS plays a critical role in the pathophysiology of sepsis. Treatment with PEI 1800-*g*-ZIF NPs and PEI 1800 reduced the percentage of cells with a high ROS level in the peritoneal cavity (Figure 5D and Figure S7). Similarly, treatment with these materials reduced the percentage of M1 polarized macrophages (Figure 5C), indicating attenuation of inflammation. We also measured the levels of proinflammatory cytokines secreted by activated immune cells including TNF-α and interleukin 6 (IL-6). Both PEI 1800-*g*-ZIF NPs and PEI 1800 reduced the serum and peritoneal TNF-α level (Figure 5E, G). Intriguingly, unlike the PEI 1800-*g*-ZIF NPs, the pure PEI 1800 increased the peritoneal and serum IL-6 levels (Figure 5F, H). It was noted that IL-6 is a key factor in the senescence secretome secreted by damaged or senescent cells in inflamed sites or neoplastic tissues,[29] therefore we speculated that although scavenging of cfDNA could inhibit IL-6 secretion by immune cells, the toxicity of free PEI 1800 to tissues could cause cell damage or senescence, resulting in increased IL-6 release.[30] The PEI 1800-*g*-ZIF NPs group showed the lowest TLR9 activation in serum, consistent with the cfDNA level in serum (Figure 5I). Since the OD value was related to SEAP expression initiated by NF-κB, we concluded that the therapeutic effect of the PEI 1800-*g*-ZIF NPs resulted mainly from scavenging of cfDNA. Although pure PEI 1800 showed identical serum cfDNA elimination, the toxicity of free PEI 1800 may cause tissue damage and morbigenous cfDNA release, which could lead to TLR9 activation.

Since multiple organ failure caused by a “cytokine storm” is the primary consequence of severe sepsis in mice,[31] histopathological and biochemical analyses were performed to determine the effect of the materials on sepsis. Based on H&E staining, leukocyte infiltration and tissue destruction were observed in multiple organs, including the lungs, kidney, heart, and liver, of the CLP group (Figure S8), characteristics typical of multiple organ injury. Pure PEI 1800 treatment showed limited protective effect on organ damage. In contrast, the PEI 1800-*g*-ZIF NPs treatment group exhibited markedly reduced inflammation. Blood biochemical analysis indexes of liver and kidney–aspartate aminotransferase (AST), blood urea nitrogen (BUN), and creatinine (CRE)–confirmed the protective effects of the PEI 1800-*g*-ZIF NPs in preventing organ failure (Figure S9).

Since TNF-α plays a major role in organ failure in the progression of sepsis, we next investigated TNF-α secretion in the liver of mice using anti-TNF-α antibodies. Strong green fluorescence was observed in the livers of untreated and PEI 1800-treated CLP mouse groups, indicating massive secretion of TNF-α. PEI 1800-*g*-ZIF NPs treatment markedly reduced TNF-α secretion in liver, consistent with the ameliorated liver damage observed in

H&E staining images (Figure S8). Collectively, treatment with pure PEI 1800 showed limited protective effect on organ damage and reduction of damage-associated indexes, despite significantly reducing serum cfDNA as well as reducing the percentage of cells with high ROS level and the percentage of M1 polarized macrophages relative to the untreated CLP group, supporting our assumption that free PEI 1800 causes high toxicity to tissues. In addition, significant inflammatory lesions were associated with administration of pure PEI 1800 but not PEI 1800-*g*-ZIF NPs, observed by characteristic histological damage and morphology differences including inflammatory cell infiltration in liver and heart at day 5 after administration, demonstrating the lower systemic toxicity of PEI 1800-*g*-ZIF NPs versus free PEI 1800 (Figure S10). These results demonstrated that the PEI-*g*-ZIF NPs exhibit more favorable therapeutic activity and lower toxicity than the soluble free PEI 1800 *in vivo*, and thus show great potential for use in the treatment of sepsis.

CONCLUSIONS

In this study, we present a novel sepsis treatment strategy that involves scavenging inflammatory circulating cfDNA by using cationic metal–organic NPs that exhibit better DNA-binding, anti-inflammatory activity, and antisepsis therapeutic activity *in vivo* than free cationic polymer. Cationic PEI 1800-*g*-ZIF NPs inhibited cfDNA-induced TLR activation and NF-κB signaling *in vitro*. An *in vivo* study showed that the PEI 1800-*g*-ZIF NPs effectively mitigated CLP-induced multiple organ damage and increased the survival rate of mice with severe sepsis, outperforming free PEI 1800. Our work provides an alternative strategy for treating severe sepsis and opens up possibilities for developing DNA scavenging therapies for other cfDNA-associated diseases.

Supplementary Material

Refer to Web version on PubMed Central for supplementary material.

ACKNOWLEDGMENTS

The authors thank the National Natural Science Foundation of China (51925305, 51873208, 51520105004, 51833010), the National Science and Technology Major Projects for Major New Drugs Innovation and Development (2018ZX09711003-012), and the Jilin Province Science and Technology Development Program (20180414027GH) for their support. Support from NIH AR073935 is also acknowledged.

REFERENCES

(1). Angus DC; van der Poll T Severe sepsis and septic shock. N. Engl. J. Med. 2013, 369, 840–851. [PubMed: 23984731]

(2). Stevenson EK; Rubenstein AR; Radin GT; Wiener RS; Walkey AJ Two decades of mortality trends among patients with severe sepsis: a comparative meta-analysis. Crit. Care Med. 2014, 42, 625–631. [PubMed: 24201173]

(3). Rhee C; Dantes R; Epstein L; Murphy DJ; Seymour CW; Iwashyna TJ; Kadri SS; Angus DC; Danner RL; Fiore AE; Jernigan JA; Martin GS; Septimus E; Warren DK; Karcz A; Chan C; Menchaca JT; Wang R; Gruber S; Klompas M Incidence and trends of sepsis in US hospitals using clinical vs claims data. Jama 2017, 318, 1241–1249. [PubMed: 28903154]

(4). Stearns-Kurosawa DJ; Osuchowski MF; Valentine C; Kurosawa S; Remick DG The pathogenesis of sepsis. Annu. Rev. Pathol.: Mech. Dis. 2011, 6, 19–48.

(5). Cohen J The immunopathogenesis of sepsis. Nature 2002, 420, 885–891. [PubMed: 12490963]

(6). Rudd KE; Johnson SC; Agesa KM; Shackelford KA; Tsoi D; Kievlan DR; Colombara DV; Ikuta KS; Kissoon N; Finfer S; Fleischmann-Struzek C; Machado FR; Reinhart KK; Rowan K; Seymour CW; Watson RS; West TE; Marinho F; Hay SI; Lozano R; Lopez AD; Angus DC; Murray CJL; Naghavi M Global, regional, and national sepsis incidence and mortality, 1990−2017: analysis for the global burden of disease study. Lancet 2020, 395, 200–211. [PubMed: 31954465]

(7). Hotchkiss RS; Karl IE The pathophysiology and treatment of sepsis. N. Engl. J. Med. 2003, 348, 138–150. [PubMed: 12519925]

(8). Riedemann NC; Guo R-F; Ward PA Novel strategies for the treatment of sepsis. Nat. Med. 2003, 9, 517–524. [PubMed: 12724763]

(9). Seymour CW; Gesten F; Prescott HC; Friedrich ME; Iwashyna TJ; Phillips GS; Lemeshow S; Osborn T; Terry KM; Levy MM Time to treatment and mortality during mandated emergency care for sepsis. N. Engl. J. Med. 2017, 376, 2235–2244. [PubMed: 28528569]

(10). Salomão R; Martins PS; Brunialti MKC; Fernandes M. d. L.; Martos LSW; Mendes ME; Gomes NE; Rigato O TLR signaling pathway in patients with sepsis. Shock 2008, 30, 73–77. [PubMed: 18704004]

(11). Van der Poll T; Van de Veerdonk FL; Scicluna BP; Netea MG The immunopathology of sepsis and potential therapeutic targets. Nat. Rev. Immunol. 2017, 17, 407–420. [PubMed: 28436424]

(12). Bosmann M; Ward PA The inflammatory response in sepsis. Trends Immunol. 2013, 34, 129–136. [PubMed: 23036432]

(13). Saukkonen K; Lakkisto P; Pettilä V; Varpula M; Karlsson S; Ruokonen E; Pulkki K Cell-free plasma DNA as a predictor of outcome in severe sepsis and septic shock. Clin. Chem. 2008, 54, 1000–1007. [PubMed: 18420731]

(14). Nishimoto S; Aini K; Fukuda D; Higashikuni Y; Tanaka K; Hirata Y; Yagi S; Kusunose K; Yamada H; Soeki T; Shimabukuro M; Sata M Activation of Toll-like receptor 9 impairs blood flow recovery after hind-limb ischemia. Front. Cardiovasc. Med. 2018, 5, 144. [PubMed: 30460242]

(15). Wittebole X; Castanares-Zapatero D; Laterre PF Toll-like receptor 4 modulation as a strategy to treat sepsis. Mediators Inflammation 2010, 2010, 1. [PubMed: 19756998]

(16). Lima CX; Souza DG; Amaral FA; Fagundes CT; Rodrigues IPS; Alves-Filho JC; Kosco-Vilbois M; Ferlin W; Shang L; Elson G; Teixeira MM Therapeutic effects of treatment with anti-TLR2 and anti-TLR4 monoclonal antibodies in polymicrobial sepsis. PLoS One 2015, 10, e0132336. [PubMed: 26147469]

(17). Solov'eva T; Davydova V; Krasikova I; Yermak I Marine compounds with therapeutic potential in gram-negative sepsis. Mar. Drugs 2013, 11, 2216–29. [PubMed: 23783404]

(18). Lee J; Sohn JW; Zhang Y; Leong KW; Pisetsky D; Sullenger BA Nucleic acid-binding polymers as anti-inflammatory agents. Proc. Natl. Acad. Sci. U. S. A. 2011, 108, 14055–14060. [PubMed: 21844380]

(19). Peng B; Liang H; Li Y; Dong C; Shen J; Mao H-Q; Leong KW; Chen Y; Liu L Tuned cationic dendronized polymer: molecular scavenger for rheumatoid arthritis treatment. Angew. Chem., Int. Ed. 2019, 58, 4254–4258.

(20). Holl EK; Shumansky KL; Borst LB; Burnette AD; Sample CJ; Ramsburg EA; Sullenger BA Scavenging nucleic acid debris to combat autoimmunity and infectious disease. Proc. Natl. Acad. Sci. U. S. A. 2016, 113, 9728. [PubMed: 27528673]

(21). Naqvi I; Gunaratne R; McDade JE; Moreno A; Rempel RE; Rouse DC; Herrera SG; Pisetsky DS; Lee J; White RR; Sullenger BA Polymer-mediated inhibition of pro-invasive nucleic acid DAMPs and microvesicles limits pancreatic cancer metastasis. Mol. Ther. 2018, 26, 1020–1031. [PubMed: 29550075]

(22). Dernedde J; Rausch A; Weinhart M; Enders S; Tauber R; Licha K; Schirner M; Zügel U; von Bonin A; Haag R Dendritic polyglycerol sulfates as multivalent inhibitors of inflammation. Proc. Natl. Acad. Sci. U. S. A. 2010, 107, 19679. [PubMed: 21041668]

(23). Gao Y; Qiao Z; Zhao S; Wang Z; Wang J In situ synthesis of polymer grafted ZIFs and application in mixed matrix membrane for CO_2 separation. J. Mater. Chem. A 2018, 6, 3151–3161.

(24). Li CL; Qin F; Li R; Zhuan J; Zhu HY; Wang Y; Wang K Preparation and in vivo expression of CS-PEI/pCGRP complex for promoting fracture healing. Int. J. Polym. Sci. 2019, 2019, 1.

(25). Zhang Z; Xian S; Xia Q; Wang H; Li Z; Li J Enhancement of CO_2 adsorption and CO_2/N_2 selectivity on ZIF-8 via postsynthetic modification. AIChE J. 2013, 59, 2195–2206.

(26). Latz E; Schoenemeyer A; Visintin A; Fitzgerald KA; Monks BG; Knetter CF; Lien E; Nilsen NJ; Espevik T; Golenbock DT TLR9 signals after translocating from the ER to CpG DNA in the lysosome. Nat. Immunol. 2004, 5, 190–198. [PubMed: 14716310]

(27). Takeshita F; Gursel I; Ishii KJ; Suzuki K; Gursel M; Klinman DM Signal transduction pathways mediated by the interaction of CpG DNA with Toll-like receptor 9. Semin. Immunol. 2004, 16, 17–22. [PubMed: 14751759]

(28). Dawulieti J; Sun M; Zhao Y; Shao D; Yan H; Lao YH; Hu H; Cui L; Lv X; Liu F; Chi C-W; Zhang Y; Li M; Zhang M; Tian H; Chen X; Leong KW; Chen L Treatment of severe sepsis with nanoparticulate cell-free DNA scavengers. Sci. Adv. 2020, 6, eaay7148. [PubMed: 32523983]

(29). Amor C; Feucht J; Leibold J; Ho YJ; Zhu C; Alonso-Curbelo D; Mansilla-Soto J; Boyer JA; Li X; Giavridis T; Kulick A; Houlihan S; Peerschke E; Friedman SL; Ponomarev V; Piersigilli A; Sadelain M; Lowe SW Senolytic CAR T cells reverse senescence-associated pathologies. Nature 2020, 583, 127–132. [PubMed: 32555459]

(30). Taranejoo S; Liu J; Verma P; Hourigan K A review of the developments of characteristics of PEI derivatives for gene delivery applications. J. Appl. Polym. Sci. 2015, 132, 42096.

(31). Chousterman BG; Swirski FK; Weber GF Cytokine storm and sepsis disease pathogenesis. Semin. Immunopathol. 2017, 39, 517–528. [PubMed: 28555385]

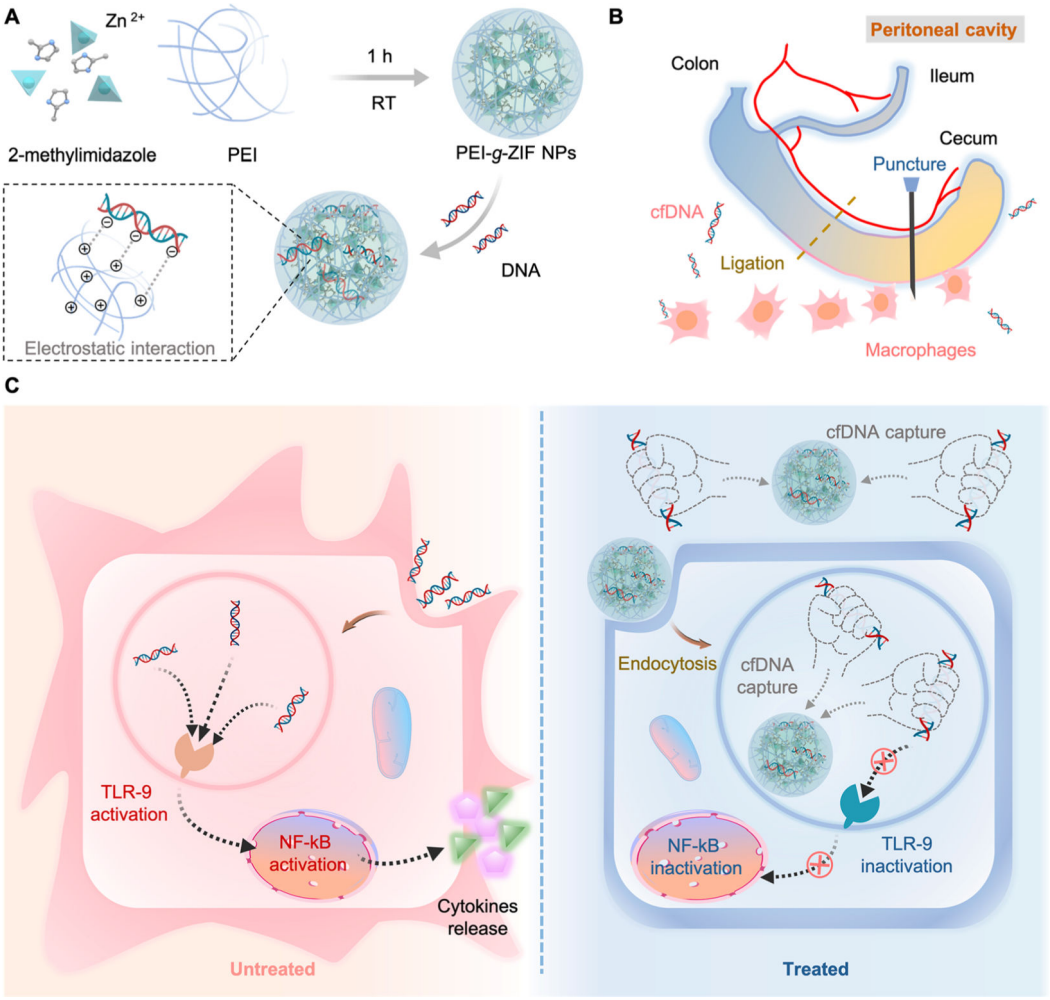

Figure 1.

(A) Preparation of PEI-*g*-ZIF NPs. (B) CLP-induced sepsis model. (C) Schematic of inflammation in untreated sepsis (left) and sepsis treatment by cfDNA scavenging by PEI-*g*-ZIF NPs (right).

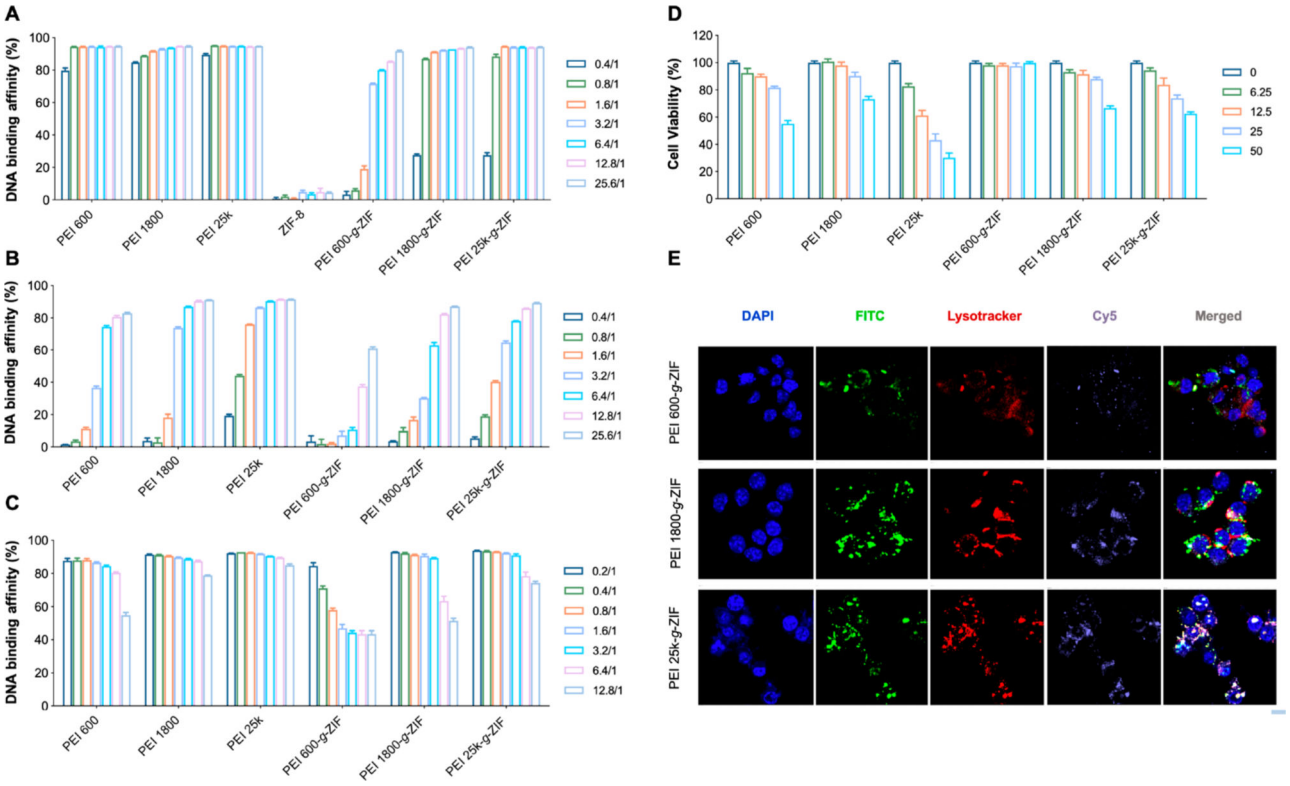

Figure 2.

DNA binding efficiency of pure PEI and PEI-*g*-ZIF NPs at various NPs:DNA mass ratios at 37 °C in (A) TE buffer and (B) TE buffer with 10% FBS. [DNA] = 0.5 μg/mL. The legends indicate NPs:DNA weight ratios. (C) DNA binding efficiency of different NPs at a weight ratio of NPs to DNA of 12.8/1 in the presence of heparin at different concentrations. [DNA] = 0.5 μg/mL. The legend indicates the heparin:DNA weight ratio. (D) Cytotoxicity of NPs at different concentrations to RAW 264.7 cells. The legend indicates NPs concentration (μg/mL). (E) CLSM images of colocalization of FITC-labeled PEI-*g*-ZIF NPs and Cy5-labeled CpG in lysosomes. Scale bar, 10 μm.

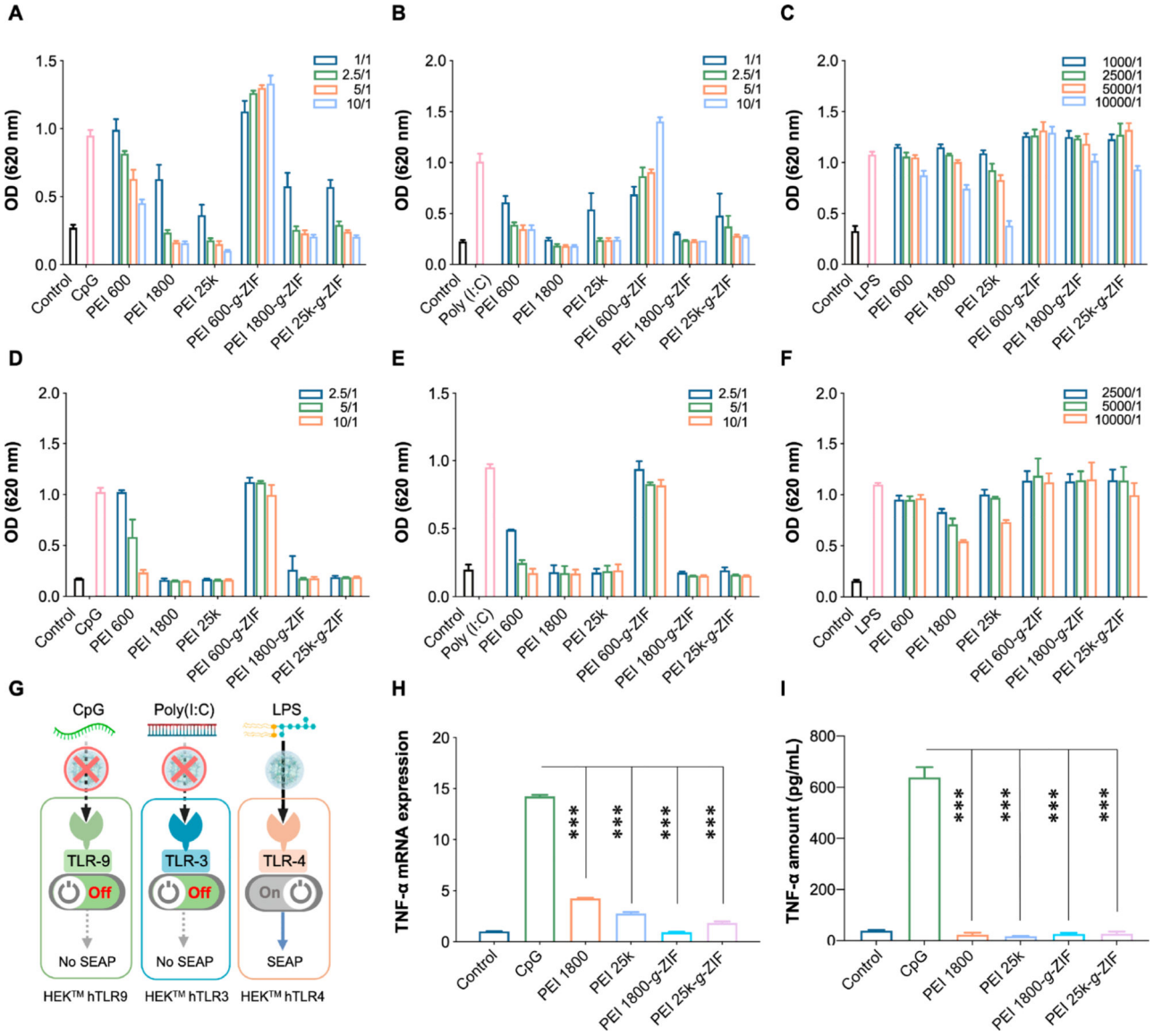

Figure 3.

Activation of (A) HEK-Blue hTLR9, (B) HEK-Blue hTLR3, and (C) HEK-Blue hTLR4 reporter cells in the absence of FBS after 24 h treatment with NPs. Activation of (D) HEK-Blue hTLR9, (E) HEK-Blue hTLR3, and (F) HEK-Blue hTLR4 reporter cells in the presence of 10% FBS after 24 h treatment with NPs. CpG DNA was added 20 min before introducing the NPs. TLR activation was determined by SEAP activity in supernatants using QUANTI-Blue (OD at 620 nm). In panels A−F, [CpG] = 1 μg/mL, [poly(I:C)] = 1 μg/mL, [LPS] = 1 ng/mL. The legend indicates NPs:agonist weight ratios. (G) Schematic of NPs inhibition of nucleic acid-induced TLR activation. (H) TNF-α mRNA and (I) TNF-α cytokine level in different groups after 24 h treatment with NPs. In all groups except the control, RAW 264.7 macrophages were stimulated with CpG for 20 min before introducing the NPs. In panel H, [CpG] = 1 μg/mL, [NPs] = 1 μg/mL. In panel I, [CpG] = 1 μg/mL; the legend indicates NPs:CpG weight ratios, and TNF-α in supernatants was evaluated by

ELISA. In panels A−I, the data are expressed as the mean ± SD. Statistical analysis of different groups was performed using Student's *t* test (*$p < 0.05$, **$p < 0.01$, ***$p < 0.001$).

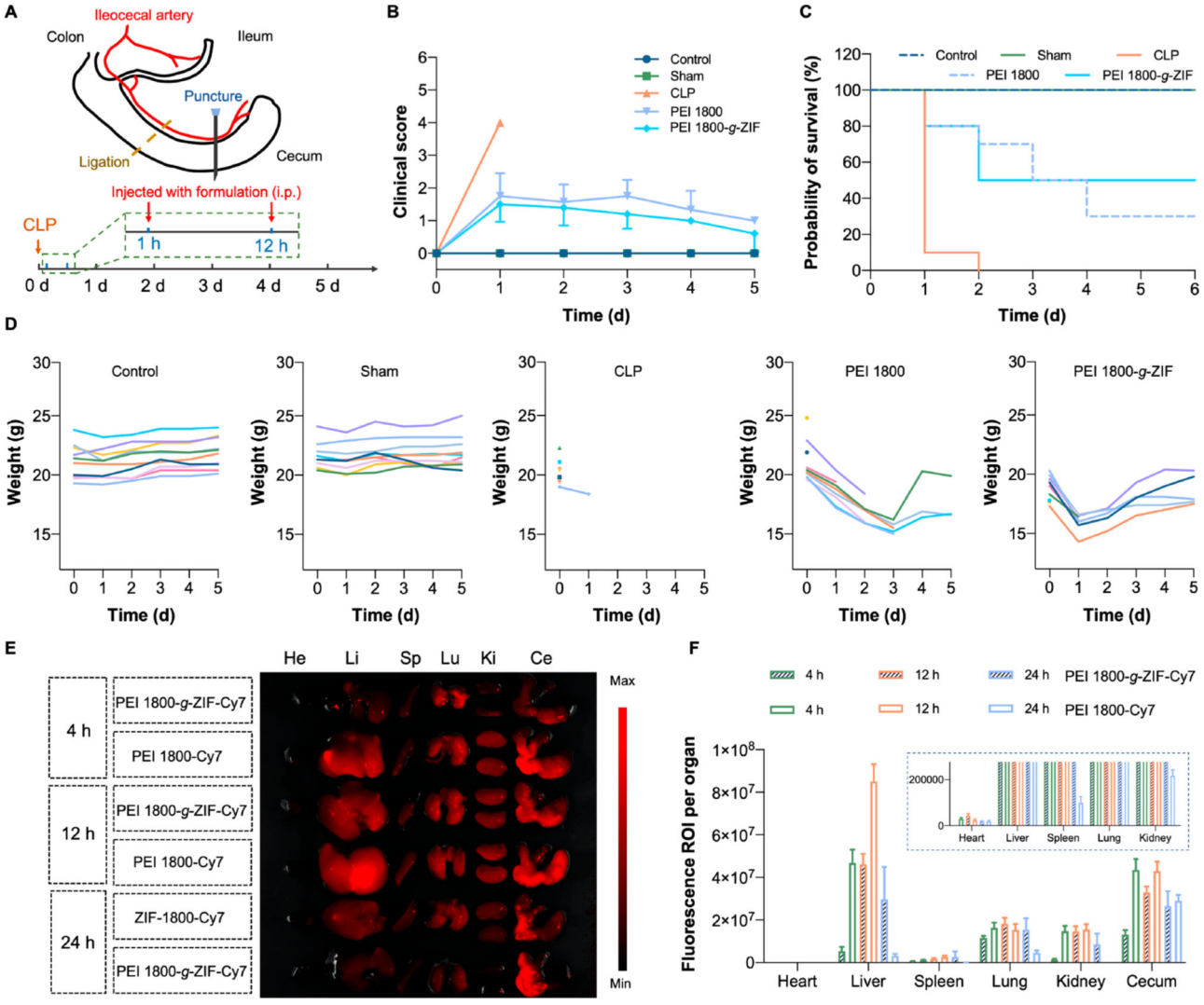

Figure 4.

(A) Schematic of establishment of CLP model and treatment schedule. (B) Clinical score, (C) survival rate, and (D) body weight of mice in different treatment groups monitored for 5 days. (E) *Ex vivo* fluorescence images and (F) quantitative data of major organs and cecum of CLP mice treated with PEI 1800-*g*-ZIF NPs and pure PEI 1800.

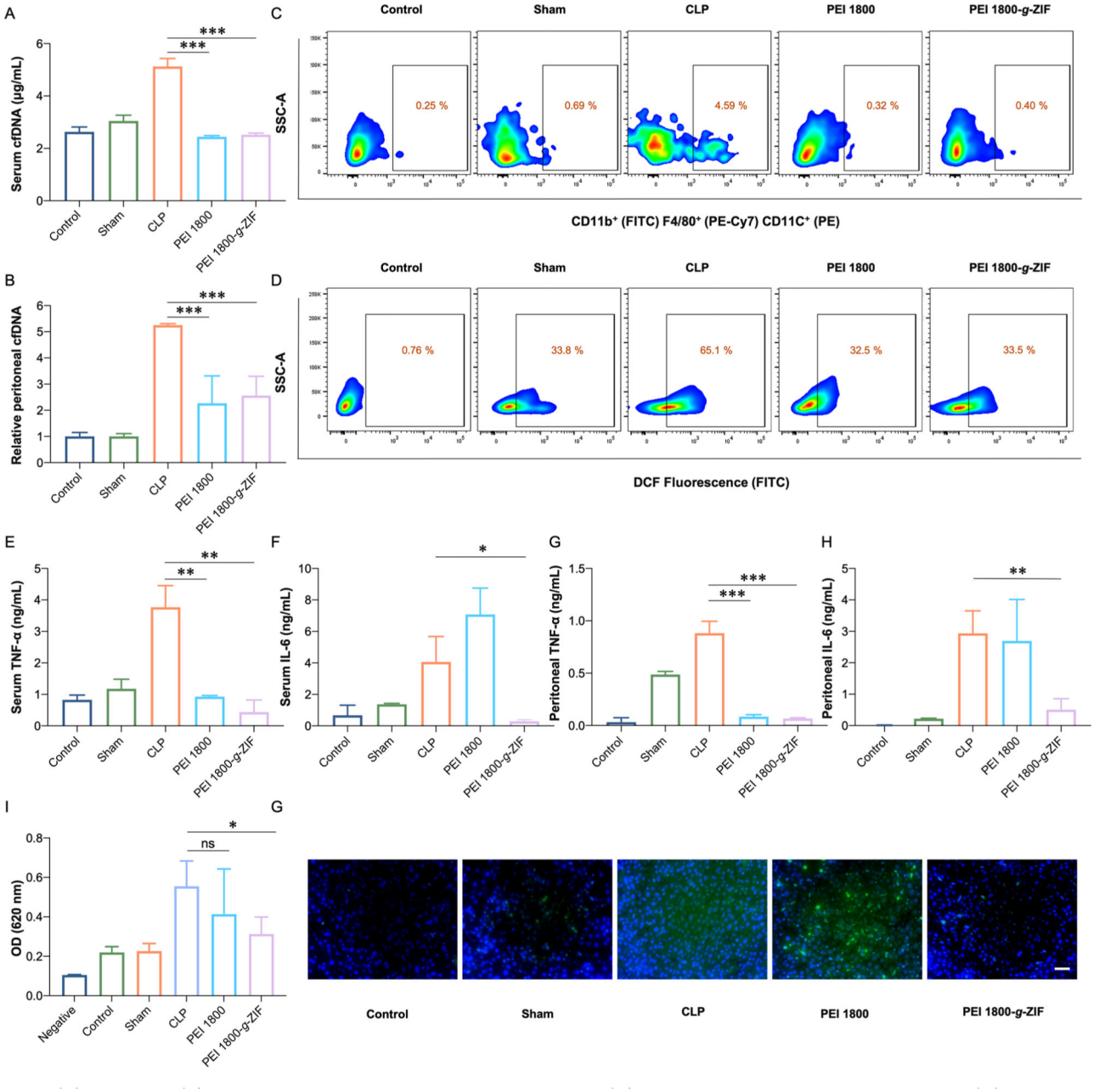

Figure 5.

(A) Serum and (B) relative peritoneal cfDNA levels at 24 h post-CLP. (C) M1 polarization ratio of macrophages and (D) cells with high ROS level in the peritoneal cavity, measured by flow cytometry at 24 h post-CLP. Proinflammatory cytokines (E) TNF-α and (F) IL-6 in serum. (G) TNF-α and (H) IL-6 in the peritoneal cavity. (I) Activation of HEK-Blue hTLR9 cells by serum of mice from different groups. (J) Fluorescence images of liver stained with anti-TNF-α. Scale bar, 50 μm. TNF-α, green; DAPI, blue. Data are expressed as the mean ± SD. Statistical analysis of groups was performed using Student's t test (*$p < 0.05$, **$p < 0.01$, ***$p < 0.001$).